

Keck Spectroscopy of Globular Clusters in the Virgo Cluster Dwarf Elliptical VCC 1386

Christopher J. Conselice^{1,2}

ABSTRACT

We present the results of a Keck spectroscopic study of globular clusters associated with the Virgo Cluster dwarf elliptical VCC 1386. We analyze blue spectroscopic absorption lines from 3500-5500 Å for 13 globular cluster candidates and confirm that five are associated with VCC 1386. By comparing metal and Balmer line indices of these globular clusters with α -enhanced single stellar population models we find that these systems are metal poor with $[\text{Fe}/\text{H}] < -1.35$ and old, with ages > 5 Gyr at 3σ confidence, placing their formation at $z \gtrsim 1$. This is one of the first spectroscopic studies of globular clusters surrounding dwarfs in a cluster, revealing that some low mass galaxies in rich environments form at least part of their stellar mass early in the history of the universe. We further find that the luminosity weighted stellar population of VCC 1386 itself is younger, and more metal rich than its globular clusters, consistent with $(V-I)_0$ colors from Hubble Space Telescope imaging. This implies that VCC 1386, like Local Group dEs, has had multiple episodes of star formation. Globular clusters associated with low luminosity systems however appear to be roughly as old as those associated with giant galaxies, contrary to the ‘downsizing’ formation of their bulk stellar populations.

1. Introduction

Galaxy formation is thought by many to be a process whereby massive galaxies are built from smaller ones. This hierarchical process is now well modeled and is a natural outcome of a lambda dominated universe with cold dark matter (e.g., Cole et al. 2000).

¹California Institute of Technology, Mail Code 105-24, Pasadena CA 91125

²National Science Foundation Astronomy & Astrophysics Fellow

Predictions based on simulations that incorporate these assumptions compare well with the large scale features of the universe measured with microwave background experiments (e.g., Spergel et al. 2003), and large scale galaxy surveys (Tegmark et al. 2004). However, there are several problems with the basic hierarchical model, mostly on the level of galaxies, and especially when predicting properties of the lowest mass systems (e.g., Moore et al. 1999). This includes predicting too many low mass companions around galaxies like our Milky Way. These models also predict too few major mergers at $z > 2$ (Conselice 2005), and have a difficult time reproducing observations of all dwarfs in rich galaxy clusters (e.g., Conselice et al. 2003a). Currently, it is assumed that differences between models and observations are due to an incomplete understanding of the physics behind star formation, although problems may also exist on a deeper more fundamental level as well.

Other tests of the hierarchical galaxy formation model are therefore needed to fully assess its assumptions and predictions. A potentially powerful way to do this is through examining low-mass galaxies, which are predicted to be, on average, the first galaxies in the universe. If the hierarchical model is correct these low-mass galaxies are possibly survivors of the merger process, and should contain some of the oldest stellar populations. Theory also predicts that the first galaxies should form in the densest environments (e.g., Springel et al. 2001; Tully et al. 2002), and thus cluster dwarf ellipticals potentially host the first stars that formed in the universe, perhaps before reionization (e.g., Bullock et al. 2000). This is particularly the case for dwarfs that exist near the center of clusters, where the oldest stars in the nearby universe are predicted to be found (White & Spergel 2000).

There is considerable evidence however that dwarf ellipticals, and lower mass galaxies in general, formed or entered clusters after the giant galaxies. For example, measurements of the integrated light in dwarf ellipticals reveal stellar population ages that are younger than the stars that make up giant ellipticals (e.g., Poggianti et al. 2001; Caldwell, Rose & Concannon 2003; Rakos & Schombert 2004). Likewise, the faint end of the red sequence in clusters is not formed until $z < 1$ (De Lucia et al. 2004). This implies that the luminosity weighted stellar populations of lower mass galaxies are younger than the stars in giant ellipticals. This would appear to be an ‘anti-hierarchical’ method of galaxy formation, such that the lowest mass systems formed after the more massive ones. This has been seen in field galaxies as well and has been described as ‘downsizing’ (Cowie et al. 1996).

Curiously, it also appears that a significant fraction of faint dEs with $M_B > -15$ originate from a process different from that which formed the brighter dEs and Es. Evidence for this includes dE radial velocity distributions similar to infalling spirals (Conselice et al. 2001), and dEs with integrated light that appear young and/or metal rich (Conselice et al. 2003a; Rakos & Schombert 2004). These dEs are potentially produced from higher mass galaxies

that became stripped of mass after infalling into clusters (e.g., Conselice 2002). However, the population of nucleated cluster dwarf ellipticals tend to have properties suggesting they are the low luminosity counterparts of giant ellipticals, such as a high globular cluster specific frequency (Miller et al. 1998). Some dEs also fall along the color-magnitude relationship, while others do not (e.g., Rakos et al. 2001; Conselice et al. 2002, 2003a). It is thus not yet clear when, or how, low mass galaxies form within a dense environment, or their relationship to dwarf galaxies in the Local Group and giant cluster ellipticals.

We address these issues by studying the stellar population properties of globular clusters surrounding a dwarf elliptical, VCC 1386, in the Virgo cluster. Globular clusters are ideal targets for this type of analysis as they can be studied as single stellar populations, and may retain clues to the earliest galaxy formation mechanisms (e.g., Forbes et al. 2004). Our target, VCC 1386, is a $M_V = -16.25$ ($\sim L_*+5$) dE with a system of globular cluster candidates, 13 of which we obtain spectroscopy for using the Keck I telescope. We confirm that five globular clusters are associated with VCC 1386, while three objects are foreground stars, with the remainder having too faint a signal to place constraints on membership. Our main conclusion is that some of the globular clusters surrounding VCC 1386 contain old and metal poor stars, in contrast to the dwarf itself, which contains a younger and more metal rich luminosity weighted stellar population. This suggests that VCC 1386 contains multiple star formation episodes, and some globulars in this system are as old as, or older than, those in giant ellipticals. Throughout this paper we use a distance to the Virgo cluster of 16.7 Mpc (Whitmore et al. 1995).

2. Observations

We selected VCC 1386 globular cluster candidates from WFPC2 Hubble Space Telescope (HST) imaging in the F555W (V) and F814W (I) bands. This imaging is from an HST dwarf elliptical galaxy snap-shot survey of the Virgo and Fornax clusters (e.g., Lotz et al. 2004). Exposure times were 2×230 seconds in the F555W band, and 300 seconds in the F814W band. For the VCC 1386 system, candidates globular clusters were selected based on having $(V-I)_0$ colors consistent with previous observations of globular clusters, with $(V-I)_0 < 1.3$. We measured magnitudes in the V and I bands for each globular cluster candidate using a $2''$ aperture with APHOT on IRAF, and corrected for galactic extinction using the reddening corrections in Schlegel et al. (1998). Based on their colors, we obtained a sample of 28 globular cluster candidates.

The spectroscopic observations we present were taken with the Keck Low Resolution Imaging Spectrometer (LRIS; Oke et al. 1995) on the Keck I telescope in February 2004.

Using one LRIS mask, we obtained spectroscopy for 13 globular cluster candidates. These clusters were located from near the center of VCC 1386, to a projected radius of 3 kpc. This system is shown in Figure 1 with the inner globular candidates with spectroscopy circled. This spectroscopy was acquired under good (seeing $\sim 0.6''$), but unphotometric conditions with a total exposure time lasting ~ 7 hours. We obtained spectroscopy with both the red and blue sides of LRIS (see Steidel et al. 2004 for a description of LRIS-B). On the blue side we utilized a 400 lines/mm grism blazed at 3400 Å, while on the red side we used the 600 lines/mm grating blazed at 5000 Å. This produced an effective resolution of 8 Å and 6 Å, respectively. The wavelength range probe was $\sim 3500 - 5500$ Å for LRIS-B, with wavelength calibration performed using HgKrXeNe comparison arc lamp spectra. The spectra was bias subtracted, flat-fielded and rectified using IRAF reduction techniques for multi-slit data, combining the various frames into a single one, and extracting the spectra for the individual globular clusters from this combination.

3. Stellar Populations of the VCC 1386 Globular Clusters

Using our spectra we identified features such as the Calcium H+K lines, Fe lines, as well as Balmer lines, such as $H\beta$, in our spectra. We derived from these lines the radial velocities of the globular clusters through cross correlating the measured absorption lines with a known early type galaxy spectrum and by identifying known lines by eye. Five of these systems (#1,2,3,4,6) (Table 1) are at the radial velocity of the host galaxy, VCC 1386, at ~ 1300 km s $^{-1}$ (Simien & Prugniel 2002). Three globular cluster candidates have radial velocities that place them within our own galaxy, and two of these are at a large projected distance from the center of VCC 1386. All of the confirmed globular clusters are within 1.5 kpc of the center of VCC 1386.

3.1. Metallicity and Age

We place constraints on the stellar populations that make up our globular cluster sample by utilizing the spectra and colors of the five confirmed members. We use Lick line indices, measured from the spectra, to determine metallicities and ages of the globular clusters (Worthey 1994; Worthey & Ottaviani 1997; Trager et al. 2000; Thomas et al. 2003), although not every absorption feature could be measured for every globular cluster. We measured the equivalent widths of the Lick indices after smoothing our spectra by a wavelength dependent Gaussian kernel to match the Lick ID resolution of ~ 9 Å (Worthey & Ottaviani 1997). Our data is not flux calibrated, but flux calibrated indices are $< 1\%$ different from

non-flux calibrated ones (e.g., Strader et al. 2003), and thus not likely contributing significantly to our error budget. We measured in our analysis the Balmer lines $H\beta$, $H\delta_F$, $H\gamma_F$, and the metal lines Fe 5270, Fe 5335 and Mg b using the updated passband and continuum wavelengths from Worthey (1994) and Worthey & Ottaviani (1997). Because we were unable to obtain Lick standard stars during our observations, we are not able to produce a direct offset between our indices and the Lick system. However using the same setup with LRIS under identical conditions these offsets are found to be smaller than the observational errors, and are not often applied (Brodie et al. 2005).

We determine the ages and metallicities of the stellar populations in our globular clusters through comparisons to Bruzual and Charlot (2003) and Thomas et al. (2003) single stellar population models. First, to constrain the ages of our globular clusters, we compare our measured Balmer indices ($H\beta$, $H\delta_F$, $H\gamma_F$) with Bruzual & Charlot (2003) models (Figure 2). The three horizontal lines in Figure 2 show the measure values of the $H\beta$, $H\delta_F$, and $H\gamma_F$ indices. The four lines over-plotted show the modeled evolution of these indices with time. While several ages are possible for the globular clusters based on these indices, they are generally consistent with being older than 5 Gyr, unless they have metallicities higher than $[\text{Fe}/\text{H}] = -0.64$, at a confidence $> 3\sigma$.

We cannot make definite conclusions regarding the ages of the globular clusters based solely on Balmer indices. However, when we compare Bruzual & Charlot (2003) models of (V–I) color and the $H\beta$ index, we find that old ages are preferred (Figure 3). Figure 3 shows the modeled evolution of (V–I) colors as a function of $H\beta$ at two different metallicities, $[\text{Fe}/\text{H}] = -1.64$ and $[\text{Fe}/\text{H}] = -0.64$. The evolution is such that that the typical globular cluster $H\beta$ value of 2.5 \AA is reached several times during the evolution of these single stellar populations (SSP). However, after about 1 Gyr, the colors of these SSP models are redder than (V–I) ~ 0.6 . This effectively limits the possibility that these globular clusters are extremely young systems, and is consistent with their being generally older than 5 Gyrs.

Constraining metallicity is also not straightforward, as most metal lines such as Mg b are influenced by the ages of stellar populations as well as by their metallicity. However by combining a metal index with a Balmer index we can constrain the luminosity weighted ages and metallicities of stellar populations. As such, we compare our measured indices to the α -enhanced SSP models of Thomas et al. (2003), using the $\alpha = 0.3$ models for the three globulars (#2,4,6) with a high enough signal to noise to accurately measure these indices. We utilize the index $\langle \text{Fe} \rangle = 0.5 \times (\text{Fe}5270 + \text{Fe}5335)$, the average of the Fe5270 and Fe5335 indices, as a measure of metallicity when compared with $H\beta$. We plot these values for our globular clusters on Figure 4a. The corresponding $H\beta$ vs. $\langle \text{Fe} \rangle$ point for the body of VCC 1386 is also plotted on Figure 4, where $H\beta = 2.21 \pm 0.24$, and $\langle \text{Fe} \rangle = 2.15 \pm 0.23$

(Geha et al. 2003).

Figure 4 shows that VCC 1386’s globular clusters are located in the low metallicity and old age part of the $H\beta$ - $\langle Fe \rangle$ diagram, with ages ~ 8 Gyr, and metallicities $[Fe/H] < -1.35$. By comparing with the Thomas et al. (2003) models, we can place statistical limits on the ages of our stellar populations. At 3σ confidence all three globulars with measured $H\beta$ and $\langle Fe \rangle$ indices are older than 5 Gyr and have a metallicity $[Fe/H] < -0.33$. When we compare the $H\beta$ and the $[\alpha/Fe]$ insensitive index $[MgFe]' = [Mg\ b \times (0.72 \times Fe5270 + 0.28 \times Fe5335)]^{1/2}$ (Thomas et al. 2003) we obtain the same constraints on ages and metallicities for globular cluster #2 (Figure 4b). We also use the M31 globular cluster relation between metallicity and $(V-I)_0$ color, $[Fe/H] = 4.22 \pm 0.39 (V-I)_0 - 5.39 \pm 0.35$ (Barmby et al. 2000) to place a photometric limit on the metallicities of these systems. Using this relationship, we find that the globular cluster metallicities vary between $[Fe/H] = -1.3$ and $[Fe/H] = -1.9$, consistent with their position on Figure 4.

Interestingly, one globular cluster (#4) has Balmer indices that are slightly larger than the other globular clusters. This globular cluster is potentially either more metal poor and as old as the others, or has a similar metallicity, but is younger. This globular is in fact located towards the center of VCC 1386 and therefore might have formed along with the bulk of the stellar populations that make up the body of VCC 1386. However, this globular cluster is not statistically inconsistent with having an old (> 8 Gyr) age and a low metallicity with $[Fe/H] < -1.7$.

Finally, in comparison to these globular clusters, the body of VCC 1386 itself has a higher $\langle Fe \rangle$ index at $\sim 5\sigma$ confidence, but a similar $H\beta$ index, giving it a higher single stellar population metallicity and a younger age (Figure 4). A comparison of the distribution of $(V-I)_0$ colors for our globular clusters and the light profile of the dE itself (Figure 5) reveals that VCC 1386’s globular clusters are more metal poor than the underlying light of VCC 1386, assuming that $(V-I)_0$ color is a tracer of metallicity. The colors of the globular clusters are in all but one case bluer than the underlying light at a given projected distance from the center of VCC 1386. If we interpret these $(V-I)_0$ colors as a metallicity indicator, then these globular clusters have a lower metallicity than the dE itself at every projected distance.

3.2. Formation Timescales with $[\alpha/Fe]$ as a constraint

Measuring the ratio of α elements to Fe, $[\alpha/Fe]$ allows us to place constraints on the star formation timescales of our globular clusters. The reason is that Type II supernovae, which

produce α elements, occur over a much quicker time-scale than Type Ia SN, which produce Iron. By examining the location of our globular clusters in a Mg b vs. $\langle\text{Fe}\rangle$ diagram, we can derive the likely values of $[\alpha/\text{Fe}]$ for our globular clusters (Figure 6). The Thomas et al. (2003) models predict that at higher α , the value of Mg b is larger at a given $\langle\text{Fe}\rangle$. The location of globular cluster #2 is consistent with a high $[\alpha/\text{Fe}]$ ratio. This is not an unambiguous result as the Thomas et al. (2003) models converge at low metallicity, and our errors are not small enough to reject lower $[\alpha/\text{Fe}]$ ratios. In contrast, the average values of Mg b and $\langle\text{Fe}\rangle$ for VCC 1087’s globular clusters place them in a low $[\alpha/\text{Fe}]$ region of Figure 6. If globular cluster #2 in VCC 1386 indeed has a high $[\alpha/\text{Fe}]$ ratio it could be either an indication that it formed in a rapid star formation event, or that the IMF of the star formation was top heavy, and more massive stars were available for producing α elements thorough Type II SN.

4. Interpretation & Discussion

Hierarchical structure formation models predict that within a given environment, the majority of the first galaxies to form should be low mass systems. Within this frame work, these low mass galaxies merge to form more massive ones. While there is evidence for the formation of galaxies through mergers at $z > 2$ (e.g., Conselice et al. 2003c), there is also evidence that lower mass galaxies continue to form their stellar populations at $z < 1$. In fact, it appears that lower mass galaxies finish forming after giants, through ‘downsizing’. This is typically found for field systems in deep optical/NIR surveys (e.g., Cowie et al. 1996; Kauffmann et al. 2003; Bundy, Ellis, Conselice 2005), although convincing evidence also exists showing that dwarf galaxies in clusters have younger light weighted stellar population ages than giant galaxies (Caldwell et al. 2003; De Lucia et al. 2004) suggesting a similar, although likely earlier, process occurring in dense environments.

Our results suggest that the globular clusters we observe in VCC 1386 are old and metal poor, and thus do not fit the downsizing picture. The reason is that because they are old and metal poor, they potentially formed earlier or at a similar time as stars in giant ellipticals. What this implies is that although downsizing is a real effect, such that some fraction of the stars in low mass galaxies form after those in giants, this does not imply that all the stars in low mass galaxies formed after most of the stars massive galaxies formed. A similar trend is seen for the Virgo dwarf VCC 1087, whose average metal indices are published in Strader et al. (2005). VCC 1087’s globular clusters have an average, and weighted standard deviation from the mean, values of $H\beta=2.35\pm0.06$, $\langle\text{Fe}\rangle = 1.17\pm0.09$ and $\text{Mg } b = 0.91\pm0.07$ (plotted on Figure 4). Globular clusters in the Fornax dwarf elliptical surrounding the Milky Way

also has similar indices (Strader et al. 2003) which are also plotted on Figure 4. This suggests that the globular clusters in dwarf ellipticals are very old (> 5 Gyr) in both the Local Group and the Virgo Cluster, two vastly different environments. This interpretation may not however be unique for globular clusters around dwarf ellipticals as Puzia et al. (2000) find metal rich globulars surrounding the dwarf NGC 3115 DW1.

Why do the integrated stellar populations in the main body of dwarf ellipticals appear to be younger than giant ellipticals, and younger than their own globular clusters? One possibility is that stellar population analyses are luminosity weighted, and are therefore sensitive to any recent star formation (Trager et al. 2000). If an equal amount of star formation were to occur in a giant and a dwarf, it would be much easier to identify these new stars in the lower mass system. We know that dwarfs in the Local group, such as the Fornax dwarf elliptical, have multiple and extended star formation episodes (Buonanno et al. 1999), including old stars (Grebel & Gallagher 2004). It is currently impossible to rule out any recent star formation in giant ellipticals that may be the counter part of the younger generations of stars that form in dwarfs after their globular clusters. GALEX observations however suggest that star formation does occur in elliptical galaxies at low redshift (Yi et al. 2005), yet the evidence for this in Virgo is currently ambiguous (Boselli et al. 2005).

If we assume that the star formation history of dwarfs in Virgo is more extended than that of the giants, the obvious question is why it continues in low-mass galaxies, but ends earlier in high mass systems. There are several possible explanations for this. One is that feedback through supernova heating is more efficient in shallower potentials (and thus lower mass galaxies). When stars first formed in a dwarf halo, supernovae and stellar winds would have been very efficient at removing and heating gas. This feedback effectively slows down the star formation process compared to the giant galaxies. Later, if this gas still resided in the halo, it would cool and form stars. Alternatively, AGN feedback is more effective in massive galaxies where massive black holes exist. This AGN feedback would deposit enough energy to the point where it could halt star formation fairly quickly (e.g., Granato et al. 2004). It is not clear however if low mass dwarf galaxies contain black holes, or go through an AGN phase, and thus it is possible that a corresponding processes in dwarfs would not be as effective.

Delayed star formation in dwarf ellipticals induced by SN feedback however presents another problem, namely why so few globulars formed during later stages of star formation. With the possible exception of globular cluster #4, it appears that all of the globulars in our sample are older and more metal poor than VCC 1386 itself. The colors of the globular clusters surrounding VCC 1386, even those for which we do not have measured indices, are furthermore bluer than the light from VCC 1386 at the same projected position. This is also

seen for the dozens of other globular cluster systems studied in the Virgo and Fornax clusters by the Hubble Space Telescope (Lotz et al. 2004). A possible explanation is that the Virgo cluster formed the bulk of its mass between the time the first globulars in VCC 1386 formed, and later star formation that formed the remainder of VCC 1386. Due to tides, the more massive cluster could have induced cluster evaporation in the lower dwarf potentials. The delay in star formation can also be accounted for by the reionization of the universe (e.g., Santos 2003) which appears to have occurred between $z \sim 6-10$. This would allow globulars to form before reionization, and any remaining gas inside these halos would photo-evaporate. Later episodes of star formation would then occur once the gas inside these lower mass halos cools, which likely occurred at $z < 1$. Cold gas is seen in roughly $\sim 15\%$ of dwarf ellipticals in the Virgo cluster (Conselice et al. 2003b), making this a possible scenario.

Finally, our results are consistent with some of the globular clusters surrounding giant ellipticals originating from dwarf ellipticals. Both color distributions and Lick indices for globular clusters surrounding giant galaxies in the Virgo cluster overlap the same values found for the globulars in VCC 1386 (e.g., Kundu et al. 1999; Cohen et al. 2002). For example, giant Virgo elliptical galaxies, such as M87, have blue color distributions that overlap the color distribution of our dE globular clusters (e.g., Kundu et al. 1999; Forbes et al. 2004; Figure 5), suggesting that giant elliptical globular clusters may have formed partially from the accretion and mergers of lower mass systems. However, it is impossible for globular clusters in dwarfs to form all the globulars around giant galaxies, as there is also a significant red globular cluster population surrounding giant ellipticals (Zepf & Ashman 1993). A speculative explanation for this is that some of these red globulars form out of cold gas transported by an accreted dwarf, the same material the body of the dwarfs we see today were formed.

More observations of globular clusters in dwarf elliptical galaxies in rich environments, such as in Virgo and Fornax, are needed to determine the universality of these results, and whether multiple populations of globular clusters with differing ages and metallicities exist within dwarfs. However, due to the faintness of these globulars, a comprehensive study likely must await the advent of 20-30 meter sized telescopes.

I thank Jason Rhodes for help with the observations, Arunav Kundu for making his list of M87 globular cluster photometry available electronically, and Jean Brodie and James Taylor for useful discussions. I also acknowledge support from an NSF Astronomy and Astrophysics Fellowship. I also wish to recognize the highly significant cultural role and reverence that the summit of Mauna Kea has within the indigenous Hawaiian community, it is a privilege to be given the opportunity to conduct observations from this mountain.

REFERENCES

- Barmby, P., Huchra, J.P., Brodie, J.P., Forbes, D.A., Schroder, L.L., & Grillmair, C.J. 2000, *AJ*, 119, 727
- Boselli, A., et al. astro-ph/0507169
- Bullock, J.S., Kravtsov, A.V., Weinberg, D.H. 2000, *ApJ*, 539, 517
- Buonanno, R., Corsi, C.E., Castellani, M., Marconi, G., Fusi Pecci, F., & Zinn, R. 1999, *AJ*, 118, 1671
- Brodie, J.P., et al. 2005, *AJ*, 129, 2643
- Bruzual, A.G., & Charlot, S. 2003, *MNRAS*, 344, 1000
- Bundy, K., Ellis, R.S., & Conselice, C.J. 2005, *ApJ*, 625, 621
- Caldwell, N., Rose, J.A., & Concannon, K.D. 2003, *AJ*, 125, 2891
- Cohen J.G., Blakeslee, J.P., & Cote, P. 2002, *ApJ*, 592, 866
- Cole, S., Lacey, C.G., Baugh, C.M., & Frenk, C.S., 2000, *MNRAS*, 319, 168
- Conselice, C.J. 2002, *ApJ*, 573, 5L
- Conselice, C.J., Gallagher, J.S., Wyse, R.F.G. 2001, *ApJ*, 559, 791
- Conselice, C.J., Gallagher, J.S., Wyse, R.F.G. 2003a, *AJ*, 125, 66
- Conselice, C.J., O’Neil, K., Gallagher, J.S., & Wyse, R.F.G. 2003b, *ApJ*, 591, 167
- Conselice, C.J., Bershadsky, M.A., Dickinson, M., & Papovich, C. 2003c, *AJ*, 126, 1183
- Conselice, C.J. 2005, astro-ph/0507146
- Cowie, L.L., Songaila, A., Hu, E.M., & Cohen, J.G. 1996, *AJ*, 112, 839
- De Lucia, G., et al. 2004, *ApJ*, 610, L77
- Forbes, D.A., et al. 2004, *MNRAS*, 355, 608
- Grebel, E.K., & Gallagher, J.S. III, 2004, *ApJ*, 610, L89
- Geha, M., Guhathakurta, P., & van der Marel, R.P. 2003, *AJ*, 126, 1794
- Granato, G., De Zotti, G., Silva, L., Bressan, A., & Danese, L. 2004, *ApJ*, 600, 580
- Kauffmann, G., et al. 2003, *MNRAS*, 341, 33
- Kundu, A., Whitmore, B.C., Sparks, W.B., Macchetto, F.D., Zepf, S.E., & Ashman, K.M. 1999, *ApJ*, 513, 733
- Lotz, J.M., Miller, B.W., & Ferguson, H.C. 2004, *ApJ*, 613, 262

- Miller, B.W., Lotz, J.M., Ferguson, H.C., Stiavelli, M., & Whitmore, B.C. 1998, *ApJ*, 508, 133L
- Moore, B. et al. 1999, *ApJ*, 524, 19L
- Oke, B. et al. 1995, *PASP*, 107, 375
- Poggianti, B.M., et al. 2001, *ApJ*, 562, 689
- Puzia, T.H., Kissler-Patig, M., Brodie, J.P., & Schroder, L.L. 2000, *AJ*, 120, 777
- Rakos, K., & Schomber, J. 2004, *AJ*, 127, 1502
- Santos, M. 2003, in “Extragalactic Globular Cluster Systems”, ed. M. Kissler-Patig, p. 348
- Schlegel, D.J., Finkbeiner, D.P., & Davis, M. 1998, *ApJ*, 500, 525
- Simien, F., & Prugniel, P. 2002, *A&A*, 384, 371
- Spergel, D.N., et al. 2003, *ApJS*, 148, 175
- Springel, V., White, S.D.M., Tormen, G., & Kauffmann, G. 2001, *MNRAS*, 328, 726
- Steidel, C.C., Shapley, A.E., Pettini, M., Adelberger, K.L., Erb, D.K., Reddy, N.A., & Hunt, M.P. 2004, *ApJ*, 604, 534
- Strader, J., Brodie, J.P., Cenarro, A.J., Beasley, M.A., Forbes, D.A. 2005, *astro-ph/0506289*
- Strader, J., Brodie, J.P., Forbes, D.A., Beasley, M.A., & Huchra, J.P. 2003, *AJ*, 125, 1291
- Tegmark, M., et al. 2004, *PhRvD*, 69, 103501
- Thomas, D., Maraston, C., Bender, R. 2003, *MNRAS*, 339, 897
- Trager, S.C., Faber, S.M., Worthey, G., Gonzalez, J.J. 2000, *AJ*, 120, 165
- Tully, R.B., Somerville, R.S., Trentham, N., & Verheijen, M.A. 2002, *ApJ*, 569, 573
- West, M.J., Cote, P., Marzke, R.O., & Jordan, A. 2004, *Nature*, 427, 31
- White, S.D.M., Springel, V. 1999, *astro-ph/9911378*
- Whitmore, B.C., Sparks, W.B., Lucas, R.A., Macchetto, F.D., & Bieretta, J.A. 1995, *ApJ*, 454, L73
- Worthey, G. 1994, *ApJS*, 95, 107
- Worthey, G., & Ottaviani, D.L. 1997, *ApJS*, 111, 377
- Yi, S.K., et al. 2005, *ApJ*, 619, 111L
- Zepf, S., & Ashman, K. 1993, *MNRAS*, 264, 611

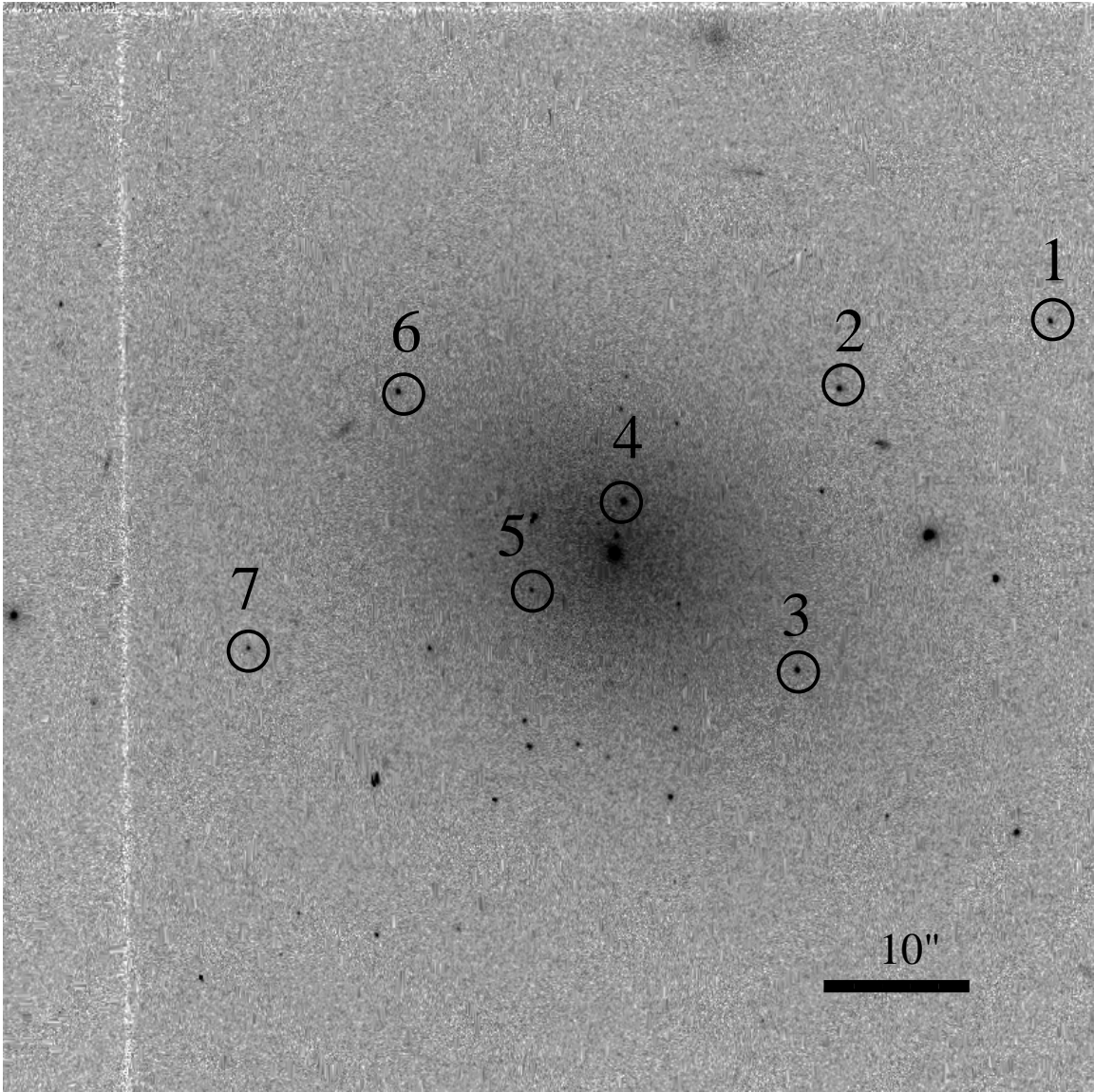


Fig. 1.— Hubble Space Telescope image of VCC 1386 with its globular clusters circled and numbered. The confirmed globular cluster members are objects #1,2,3,4,6.

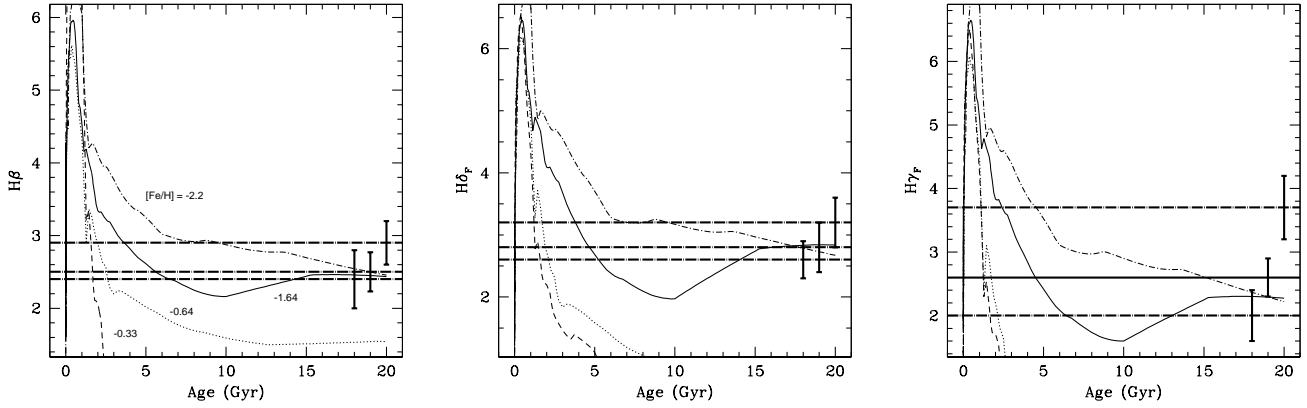


Fig. 2.— A comparison between the Balmer indices for our globular clusters ($H\beta$, $H\delta_F$ and $H\gamma_F$ plotted as horizontal lines) and models of how these indices evolve as a function of time from Bruzual & Charlot (2003). Four models are plotted at metallicities $[\text{Fe}/\text{H}] = -2.2$, -1.64 , -0.64 and -0.33 , from top to bottom, respectively. Error bars for these indices are plotted on the right hand side at arbitrary chosen ages of 20, 19 and 18 Gyr.

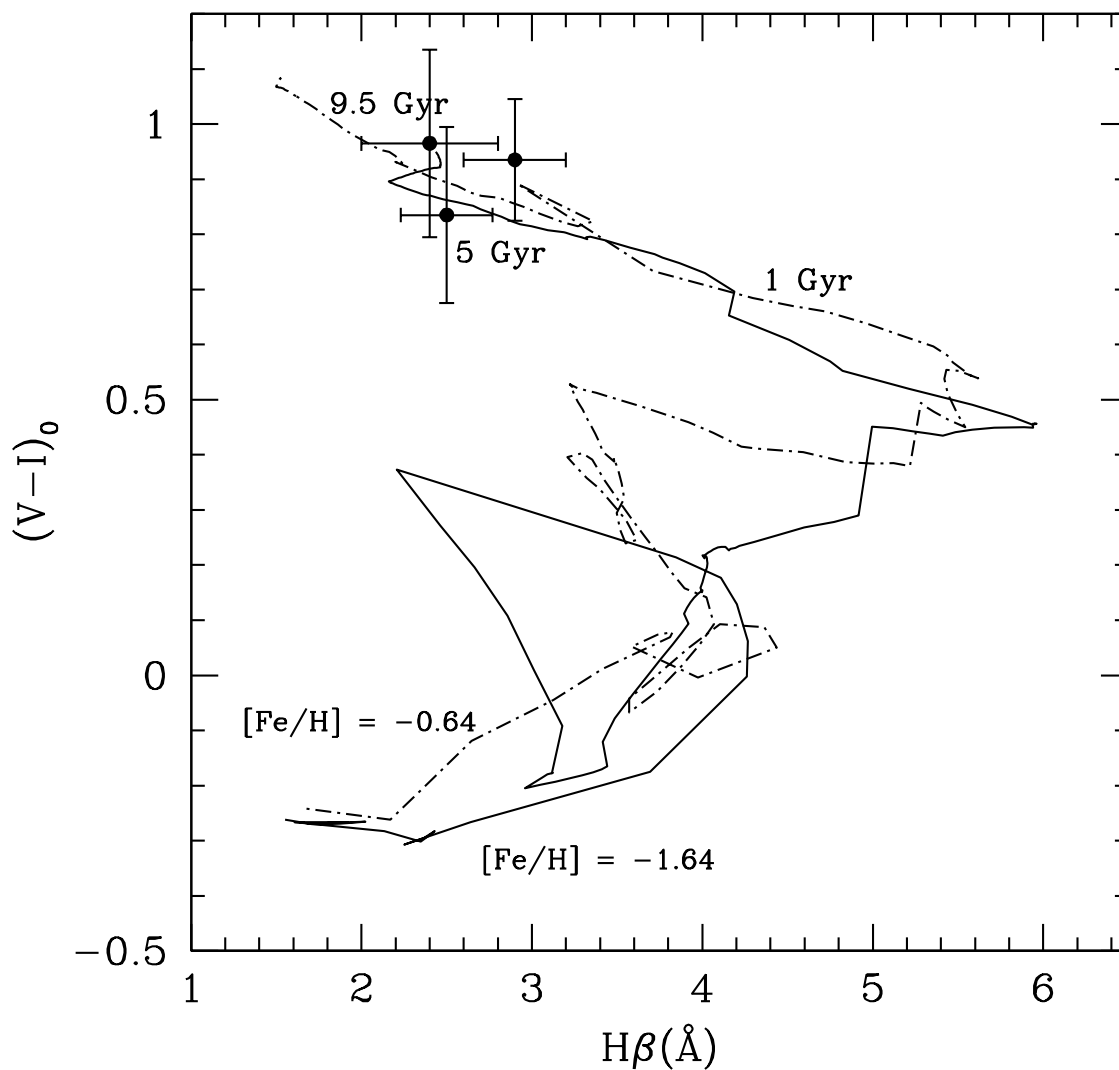


Fig. 3.— Plot of $(V-I)$ colors and the $H\beta$ index for VCC 1386’s globular clusters. Two Bruzual & Charlot (2003) evolutionary models at metallicities $[Fe/H] = -1.64$ and -0.64 are over plotted. Other metallicities, such as $[Fe/H] = -2.2$ and $[Fe/H] = -0.33$ show a similar evolution. The three points with error bars represent the values for our globular clusters. The average position on this diagram where modeled ages reach 1 Gyr, 5 Gyr and 9.5 Gyr are labeled.

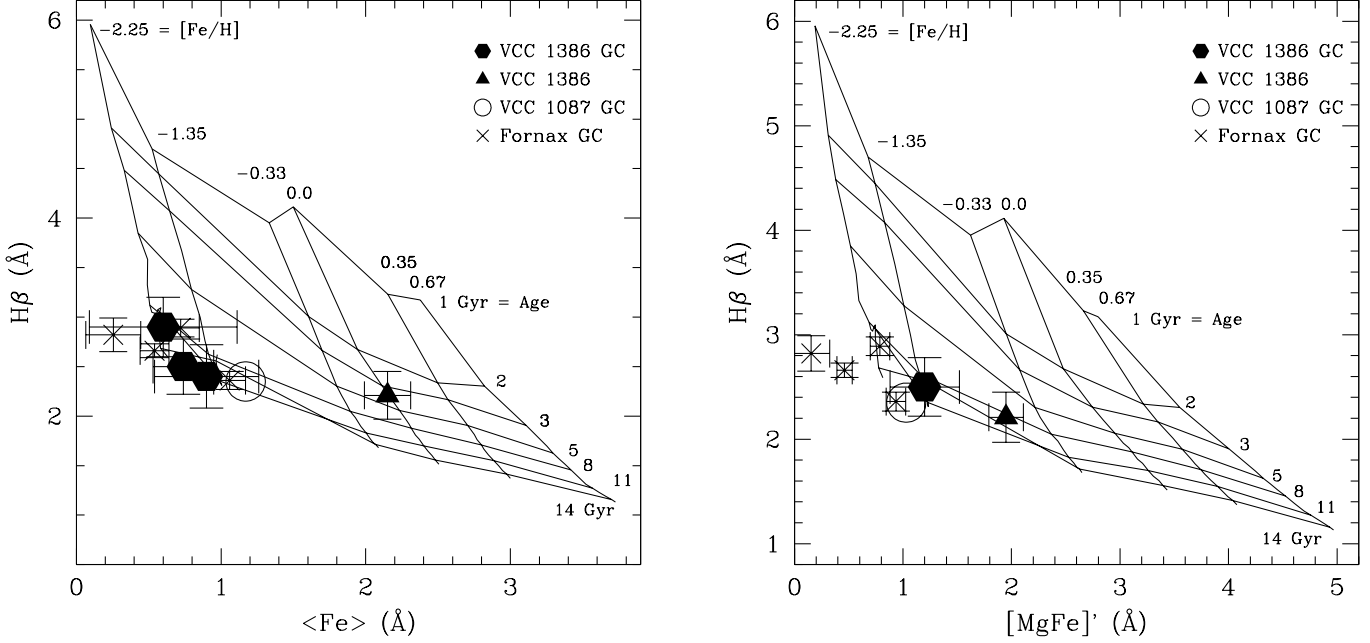


Fig. 4.— (a) Plot of the indices $H\beta$ and $\langle Fe \rangle$ for the VCC 1386 globular clusters (hexagons) superimposed on Thomas et al. (2003) model isochrones and isometallicity lines for $[\alpha/Fe] = 0.3$. The different ages and metallicities along this grid are labeled. Indices for the body of VCC 1386 is shown as a triangle (Geha et al. 2003). Values for the globular clusters surrounding the Local Group dwarf elliptical Fornax are plotted as crosses (Strader et al. 2003), while the average values for the globular clusters surrounding the Virgo dE VCC 1087 is plotted as an open circle (Strader et al. 2005). (b) Similar to (a) except the index $[MgFe]'$ (see text) is plotted with $H\beta$.

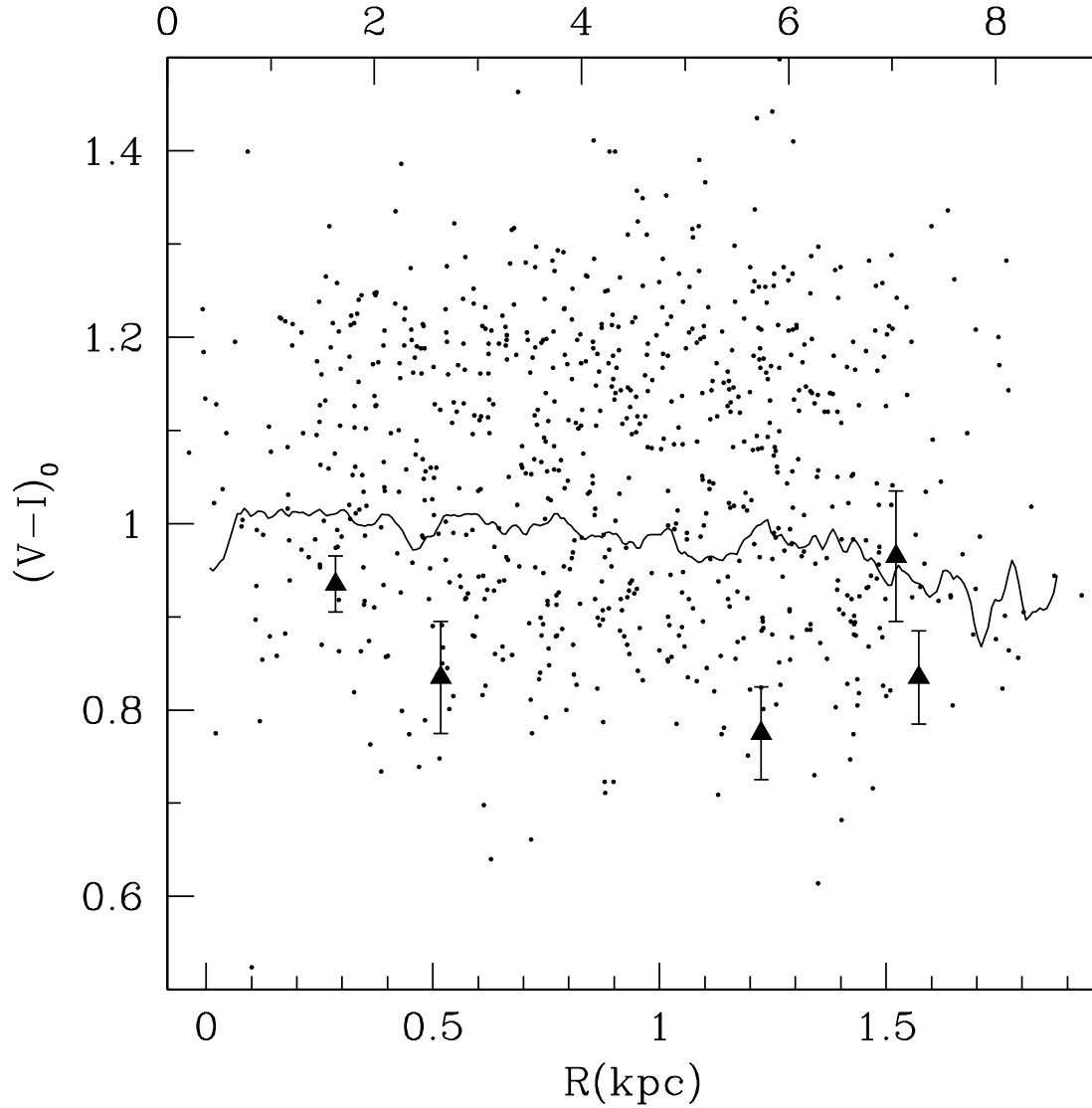


Fig. 5.— The radial distribution of VCC 1386 globular cluster colors (triangles). The solid line is the color profile for VCC 1386. The small points and top axis give the radial distribution of colors for ~ 800 inner globular clusters surrounding M87 out to ~ 8 kpc (Kundu et al. 1999).

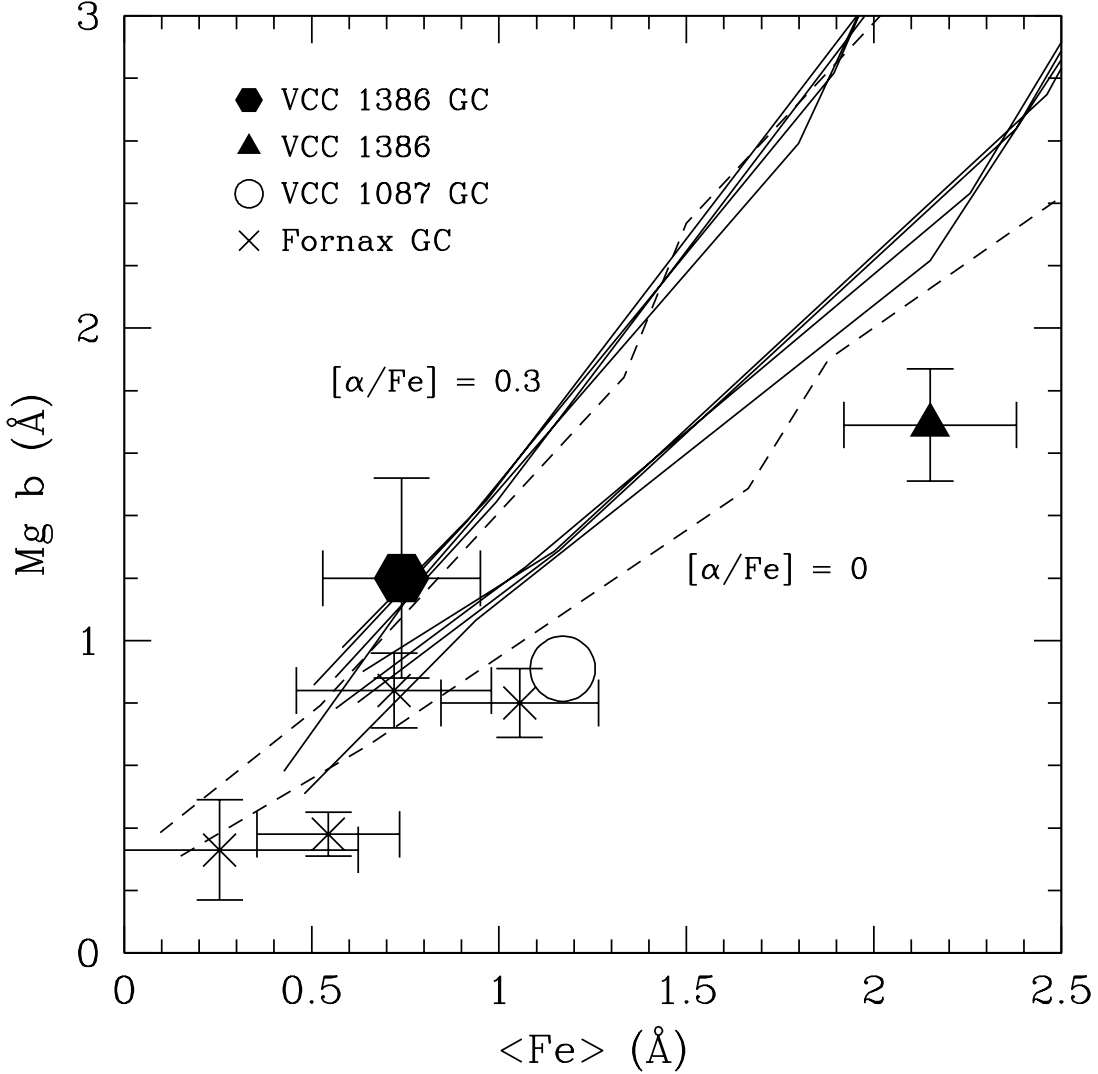


Fig. 6.— Figure showing the relationship between the $\langle \text{Fe} \rangle$ index and the $\text{Mg } b$ index for globular cluster #2. Also plotted are the same indices for globulars found in the Fornax dE, the average values for globulars in another Virgo dwarf elliptical, VCC 1087 (Strader et al. 2005), and the value for the body of VCC 1386. Models are over-plotted as lines showing the relationship between $\langle \text{Fe} \rangle$ and $\text{Mg } b$ at two different values of α ($\alpha=0.3$ and $\alpha=0$). The individual model lines show this relationship at ages 1,5,8,11 and 14 Gyr, where the youngest age, 1 Gyr, is plotted as the dashed line at each α value.

TABLE 1
 PROPERTIES OF GLOBULAR CLUSTERS AROUND VCC 1386

Number	r.a.	Dec.	V	(V-I)	H β	H δ_F	H γ_F	Mg <i>b</i>	<Fe>	[MgFe]'
1	12:31:50.7	12:38:48.7	22.8 \pm 0.12	0.97 \pm 0.32
2	12:31:50.8	12:39:05.5	22.6 \pm 0.05	0.87 \pm 0.16	2.5 \pm 0.27	3.2 \pm 0.4	2.0 \pm 0.4	1.3 \pm 0.2	0.74 \pm 0.2	1.2 \pm 0.3
3	12:31:52.1	12:39:13.3	22.3 \pm 0.05	0.81 \pm 0.15
4	12:31:51.1	12:39:23.3	21.9 \pm 0.03	0.97 \pm 0.11	2.9 \pm 0.3	2.8 \pm 0.4	3.7 \pm 0.5	...	0.7 \pm 0.5	...
6	12:31:50.3	12:39:38.1	22.6 \pm 0.07	1.00 \pm 0.17	2.4 \pm 0.4	2.6 \pm 0.3	2.6 \pm 0.3	...	0.9 \pm 0.4	...